Indian Journal of Science and Technology Vol.2 No. 9 (Sep 2009) ISSN: 0974- 6846

Vibration analysis of misaligned shaft –ball bearing system

V. Hariharan[1] and PSS. Srinivasan[2]
[1] *Dept. of Mech. Engg., Kongu Engg. College, Perundurai, Erode- 638052, India.*
[2] *Knowledge Institute of Technology ,Salem, 637504, India.*
harimech@rediffmail.com, hariharan_vag@yahoo.com, pssmech@yahoo.com

Abstract: Experimental studies were performed on a rotor dynamic test apparatus to predict the vibration spectrum for shaft misalignment. A self-designed simplified 3 pin type flexible coupling was used in the experiments. The rotor shaft accelerations were measured using dual channel vibration analyzer (ADASH) under the misalignment condition. The experimental and numerical (ANSYS) frequency spectra were obtained. The experimental predictions are in agreement with the ANSYS results. Both the measured and ANSYS results spectra shows that misalignment can be characterized primarily by 2X (two times) shaft running speed. However, misalignment 2X is not close enough to one of the system natural frequencies to excite the system appreciably. Therefore, there are cases where the misalignment response is hidden and does not show up in the vibration spectrum. On the other hand, if 2x shaft running speed is at or close to one of the system natural frequencies, the misalignment effect can be amplified and the speed is pronounced in the frequency spectrum.

Keywords: Misalignment, vibration analysis, pin type flexible coupling, ball bearing

Introduction

Misalignment is the most cause of machine vibration. Understanding and practicing the fundamentals of rotating shaft parameters is the first step in reducing unnecessary vibration, reducing maintenance costs and increasing machine uptime.

In Industry 30% of the machine's down time is due to the poorly aligned machine. Rotor shaft misalignment is the common problem in the operation of rotating machinery and is the heart of any industry, yet it remains incompletely understood. Despite the rapid increase in understanding of rotor dynamics, no satisfactory analysis explains the range of observed phenomena. Considering the importance of the misalignment in the shaft, detecting and diagnosing the misalignment is still elusive. Vibration in rotating machinery is mostly caused by unbalance, misalignment, mechanical looseness, shaft crack and other malfunctions. Vance (1988) and Goodman (1989) observed that misalignment is present due to improper machine assembly and some time thermal distortion of the bearing housing supports, resulting in abnormal rotating preload. However, the perfect alignment between the driving and driven shafts cannot be attained. Gibbons (1976) and Arumugam *et al.* (1995) modeled the reaction forces and moments of misaligned flexible coupling;

Fig.1. Pin type coupling with shaft and key (A) Experimental set up of pin type flexible coupling (B) A- D.C Motor, B- Bearing Support, C- Coupling, D- Disk, E- Rotor Shaft, F- Base, G- Rubber, H- Ball Bearing, J- Piezo accelerometer, K- Vibration analyzer , L- Computer

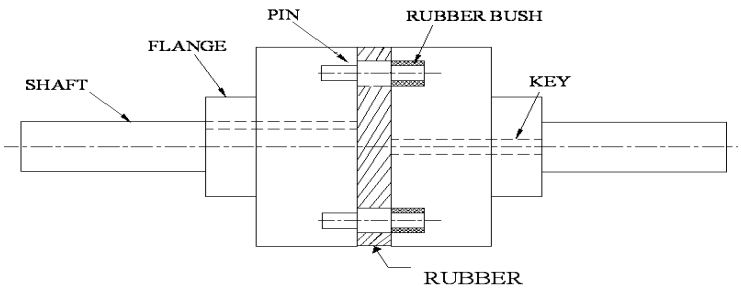

Fig. 2. Meshed rotor system

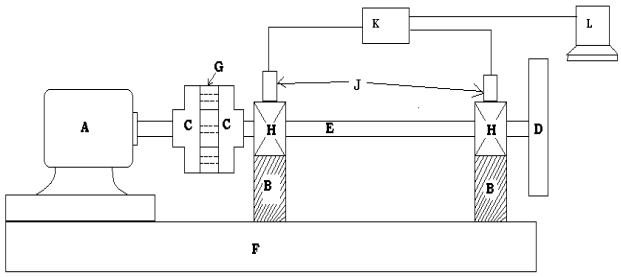

Fig.3. Rotor system with boundary conditions

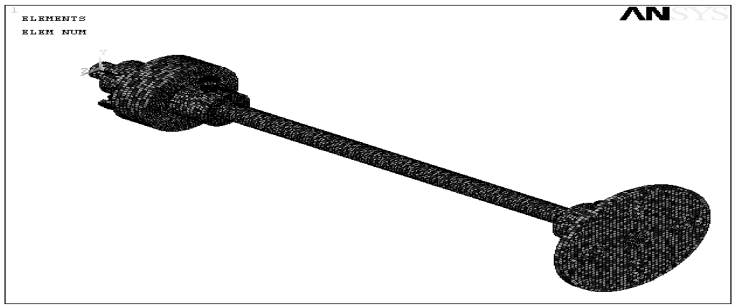

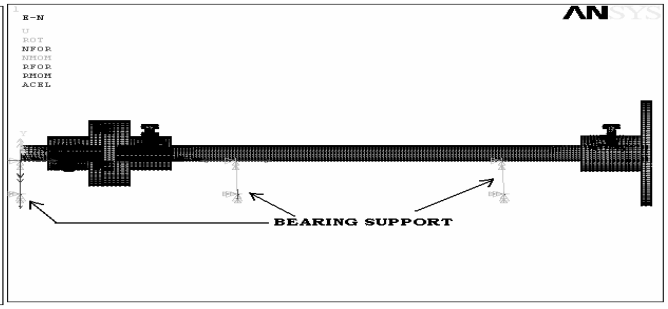

Indian Journal of Science and Technology Vol.2 No. 9 (Sep 2009) ISSN: 0974- 6846

Sekhar and Prabhu (1995) numerically evaluated the effects of coupling misalignment on the 2X vibration response of rotor-coupling- bearing system. Dewell and Mitchell (1984) showed experimentally that 2X and 4X vibration components are largely dependent upon coupling misalignment. Xu and Marangoni (1994a,b) showed that the vibration responses due to coupling misalignment mainly occur at the even multiples of the rotational speed. Simon (1992) evaluated the effect of the coupling misalignment on the bearing vibration, adapting arithmetically the exciting forces or moments due to the misalignment.

From the literature it is clearly understand that misalignment produces significant vibration levels in the bearings. It is strongly influenced by machine speed and stiffness of the coupling. Softer coupling are more forgiving, and tend to produce very less amount of vibration levels. Single point vibration spectrum for a given operating speed does not provide a reliable indication of misalignment. A machine can have parallel misalignment without exhibiting significant 2X vibration levels observed by Simon (1992) and Piotrowski (2006). Vibration due to misalignment is usually characterized by a 2X running speed component and high axial vibration levels. When a misaligned shaft is supported by rolling-element bearing, these characteristic frequencies may also appear.

In this study, a newly designed pin type of flexible coupling is used for simulation using ANSYS by introducing the bearing and coupling elements in to the model as the misalignment effects. The same is also performed experimental studies to investigate the rotor dynamics characteristics related to misalignment and to verify the numerically developed misaligned rotor systems.

Table 1. Dimension of the shaft and coupling

Description	*Unit*
Shaft diameter	19 mm
Length of the Shaft	466 mm
Hub diameter	40 mm
Length of the hub	30 mm
Outside diameter of flange coupling	80 mm
Number of holes for pin	3
Diameter of pin hole	11 mm
Diameter of pin	6 mm
Rubber bush diameter Outside diameter Inside diameter	 11 mm 6 mm
Keyway Depth	
In shaft In hub	3.5 mm 2.8 mm
Keyway cross section	
Height Width	6 mm 6 mm

Table 3. Mooney Rivlin constants

C_1	C_2	C_3	C_4	C_5	C_6	C_7	C_8	C_9
58.66	0.774	54.26	-117.49	52.77	3.58	-23.067	33.69	-12.486

Table 2. Material properties

Properties	Cast-iron	Mild steel	Rubber
Young's modulus, (MPa)	1×10^5	2×10^5	30
Poisson ratio	0.23	0.3	0.49
Density, (kg/mm^3)	7250×10^{-9}	7850×10^{-9}	1140×10^{-9}

Description of pin type coupling

The newly designed coupling is shown in Fig.1(A). It has two flanges. One flange has a pin hole of required number at pitch circle diameter. Other flange will have a number of pins projected out side at pitch circle diameter to accommodate in to the first flange hole with rubber bush. The driver and driven shafts are connected to their respective flanges i.e. output and input flanges by means of parallel square key. Mild-steel is considered for the input and output shafts, pins and keys. Over this pin, a circular natural rubber bush is provided and its length is equal to the length of the hole. The diameter of the flange holes is equal to the diameter of pin plus the thickness of rubber bush.

The cast-iron material is chosen for both left and right flanges and the natural rubber is for bush. There is no nut and bolt to clamp the both input and output flanges. In between flanges a rubber material is introduced to give the flexibility.

Description of the experimental setup

The experimental apparatus is shown in Fig.1(B). It consists of a D.C motor, a flexible coupling and a single disk rotor. The rotor shaft is supported by two identical ball bearings and has a length of 466 mm with a bearing span of 197 mm. The diameter of the rotor shaft is 19 mm. A Disk of 128 mm in diameter and 7 mm in thickness is mounted on the rotor shaft non drive end. The bearing pedestals are adjustable in vertical direction so that different misalignment conditions can be created. The rotor shaft is driven by 0.75 hp D.C motor. The D.C voltage controller is used to adjust the power supply so that motor speed can be continuously increased or decreased in the range from 0 to 2000 rpm. Two dial gauge method is used to correct the shaft misalignment and base line signal has been measured at four different speeds 500, 1000, 1500 and 2000 rpm to check the concentricity.

After this a misalignment of 0.2 mm is created and measured using the dial test indicator. Signals are acquired using the accelerometer and dual channel analyzer at both the drive end and non-drive end. Signals are experimentally measured at four different speeds. The coupling is modeled and the same working condition is simulated in the FEA using ANSYS and compared the results.

The instruments used in the experiments include accelerometers and dual channel vibration analyzer. The accelerometer is calibrated with the help of calibration test accelerometer fitted with the electro dynamic shaker with power amplifier under known frequency and amplitude. The acceleration amplitude of the electro dynamic shaker is compared with that of the acceleration amplitude of the accelerometer to be calibrated. Two

Indian Journal of Science and Technology Vol.2 No. 9 (Sep 2009) ISSN: 0974- 6846

acceleration amplitudes are found to be the same. The accelerometer directly measures the acceleration of bearing housing vibration and displays in the vibration analyzer.

Finite element modeling and assumptions

Geometric dimensions and material properties: The three dimensional model of the rotor and coupling modelled by Pro/Engineer wildfire with the exact dimensions used in the experimental setup. The dimensions and the material properties are shown in the Table 1 & 2. The material property of rubber is initially defined as an isotropic material with young's modulus and poison's ratio value. In this stage the rubber is act as linear material. To convert it in to nonlinear material hyper elastic property with Mooney Rivlin constants is introduced. There are several Mooney Rivlin constants are available. In this the most accurate method is 9 constant methods. The Mooney Rivlin constants are given in the Table 3. These constants are responsible for non linear linear property of the natural rubber. The surface to surface contact is considered for rubber and cast iron flange.

Meshing Formulation

Before meshing the model, and even before building the model, it is important to think about whether a free mesh or a mapped mesh is appropriate for the analysis. A free mesh has no restrictions in terms of element shapes, and has no specified pattern applied to it. A mapped mesh is restricted in terms of the element shape it contains and the pattern of the mesh. A mapped area mesh contains either only quadrilateral or only triangular elements, while a mapped volume mesh contains only hexahedron elements. In addition, a mapped mesh typically has a regular pattern, with obvious rows of elements. In this type of mesh, first build the geometry as a series of fairly regular volumes and/or areas that can accept a mapped mesh.

In this model, the mapped mesh has been used with the element type of SOLID 95. The smart element size control is used for mapped mesh. SOLID95 is a higher order version of the 3D 8-node solid element SOLID45 Meshed model is as shown in Fig. 2. It can tolerate irregular shapes without the loss of accuracy. SOLID95 elements have compatible displacement shapes and are well suited to model curved boundaries.

Boundary conditions and loading

The rotor shaft is supported by two identical ball bearings and has a length of 466 mm with a bearing span of 197 mm. The bearing P204 type is represented by COMBIN 40 Element and the stiffness of the bearing is $1.5X10^4$ N/mm. The Fig.3 shows the boundary conditions. The rotor shaft model rotates with respect to Global Cartesian X-axis. The angular velocity applied with respect to X-axis. The degree of freedom of UX, UZ, ROTY, ROTZ are fixed at bearing ends.

Results and discussion

Frequency spectrum of baseline condition

The measured and predicted frequency spectra were obtained for baseline case. The perfect alignment cannot be achieved in practice. The same is true for rotor unbalance. Thus, a baseline case is presented first to show the residual misalignment. The measured acceleration of an aligned and balanced system with the self designed 3 pin type coupling at a speed of 8.33 Hz, 16.67 Hz, 25 Hz and 33.333 Hz (500, 1000, 1500, 2000 rpm) is shown in Fig.4-7. The baseline spectrum is measured experimentally using dual channel vibration analyzer and the numerical results (ANSYS) are compared in the Table 4.

Table 4. Acceleration (m/sec^2) values at different speeds (base line case)

RPM	Experimental Results						ANSYS Results					
	Drive End			Non Drive End			Drive End			Non Drive End		
	1x	2x	3x	1x	2x	3x	1x	2x	3x	1x	2x	3x
500	0.0125	0.015	0.016	0.02	.025	.021	0.012	0.015	0.021	0.014	0.02	0.024
1000	0.035	0.036	0.031	0.048	0.045	0.043	0.024	0.03	0.026	0.03	0.04	0.044
1500	0.03	0.039	0.049	0.039	0.049	0.055	0.039	0.049	0.042	0.039	0.045	0.055
2000	0.05	0.052	0.062	0.065	0.069	0.079	0.049	0.052	0.063	0.059	0.062	0.077

The baseline case at 500 RPM has three small spikes in the frequency spectrum at about 8 Hz, 16.3 Hz and 24.9 Hz shown in Fig.4 (A). The drive and non drive end bearing spectrum are measured. It is observed that both drive end and non end drive spectrum of experimental vibration amplitude are very close agreement with the numerical spectrum shown in Fig.4 (B). Fig.5-7 shows the base line vibration spectrum of experimental and numerical frequency spectrum at speeds 1000, 1500 and 2000 rpm. From the vibration spectrum it is observed that the coupling has to produce very little amount of vibration acceleration at different speeds. So initially the coupling arrangement is tested for its normal condition.

Frequency spectrum of misalignment of 0.2 mm condition

Misalignment is studied by setting a parallel misalignment. Parallel misalignment is given to one of the shaft. The maximum parallel misalignment that can be created in the rotor dynamic test apparatus shown in Fig.2 was 0.1 to 0.3 mm. Misalignment of 0.2 mm was introduced between the shafts. The vibration measurement has been carried out. The shaft running speed is 8.33 Hz, 16.67 Hz, 25 Hz and 33.333 Hz (500, 1000, 1500, 2000r.p.m) and the parallel misalignment is 0.2 mm. The experimental and numerical frequency spectra of misalignment cases are shown in Fig. 8-11.

Indian Journal of Science and Technology Vol.2 No. 9 (Sep 2009) ISSN: 0974- 6846

Frequency spectrum of base line condition: Experimental (A) Numerical (B)

A *Fig. 4. (at 500 rpm)* *B*

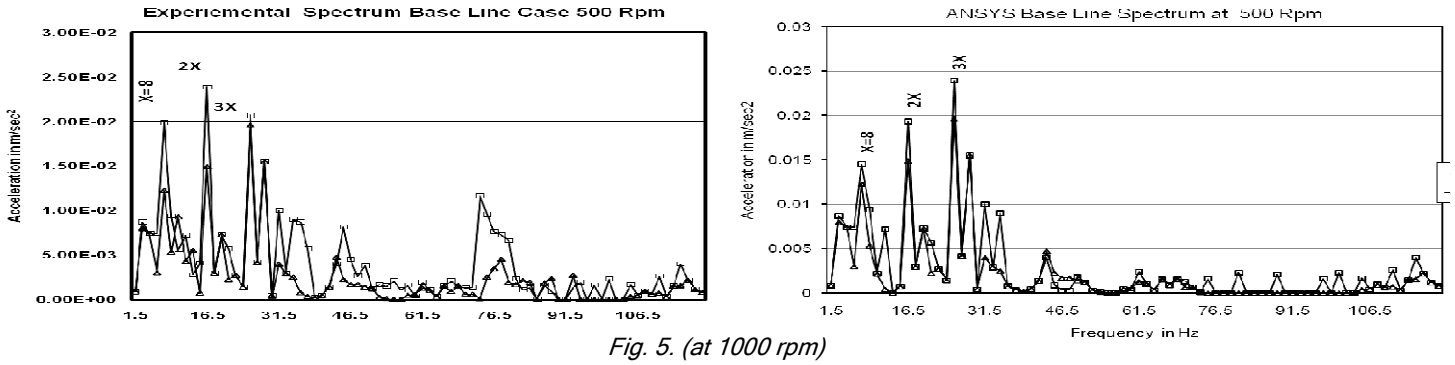

Fig. 5. (at 1000 rpm)

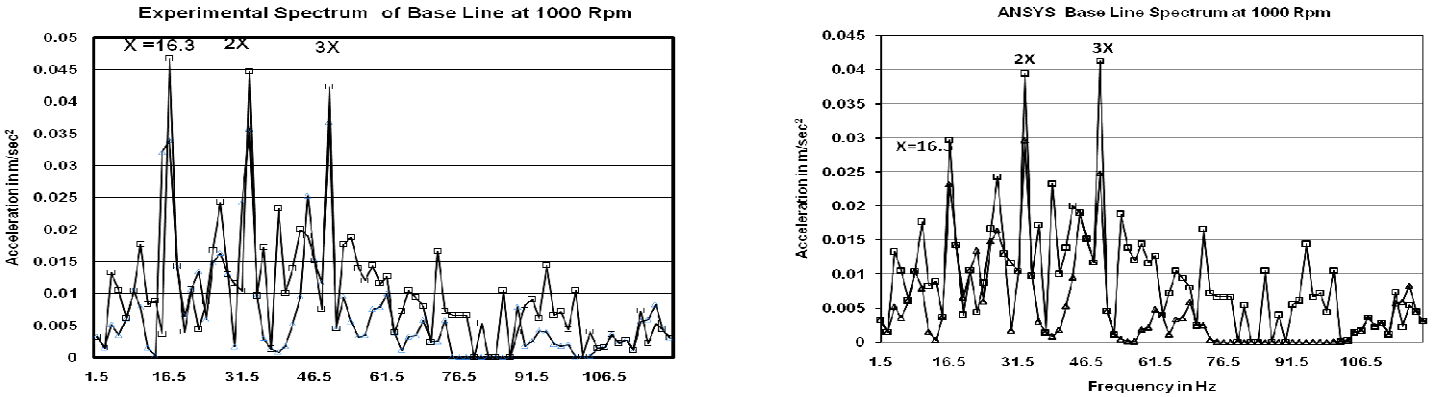

Fig.6. (at 1500 rpm)

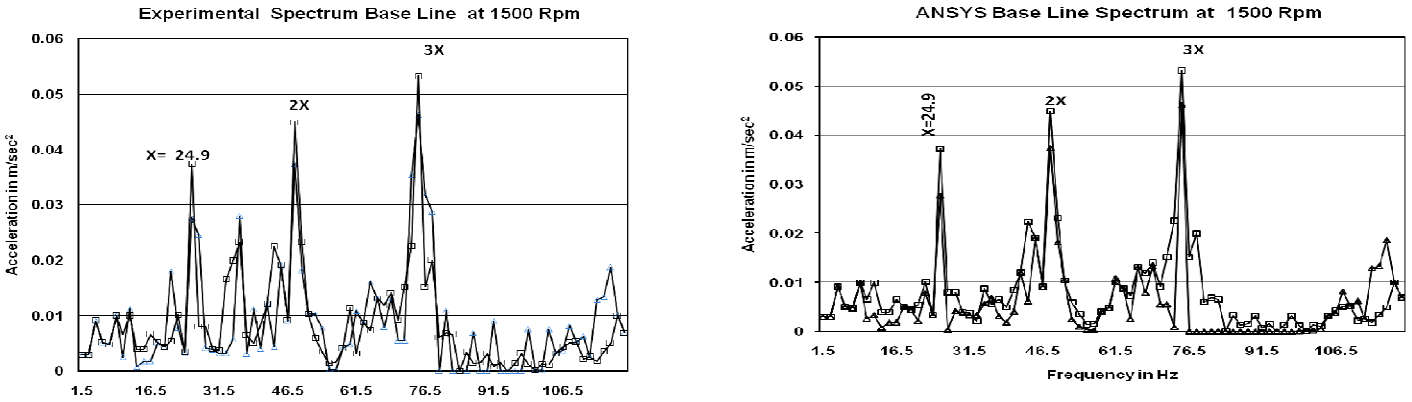

Fig.7. (at 2000 rpm)

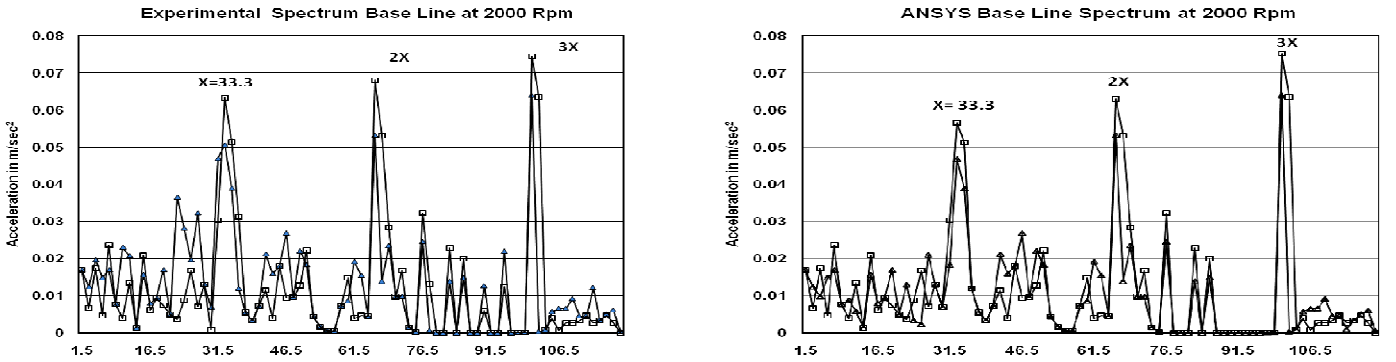

Indian Journal of Science and Technology Vol.2 No. 9 (Sep 2009) ISSN: 0974- 6846

Frequency spectrum of misalignment of 0.2 mm: Experimental (A) Numerical (B)

A *Fig. 8. (at 500 rpm)* *B*

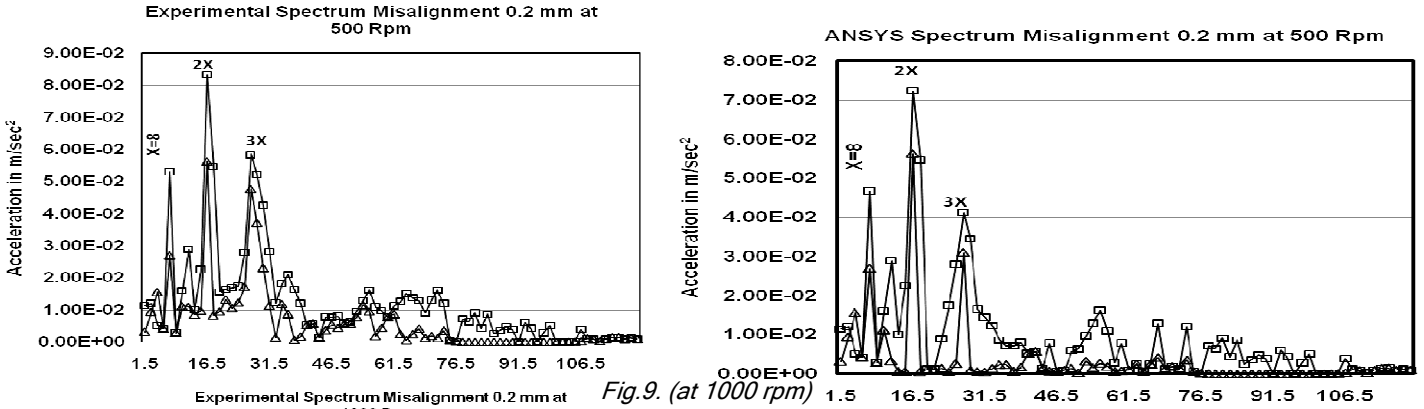

Fig.9. (at 1000 rpm)

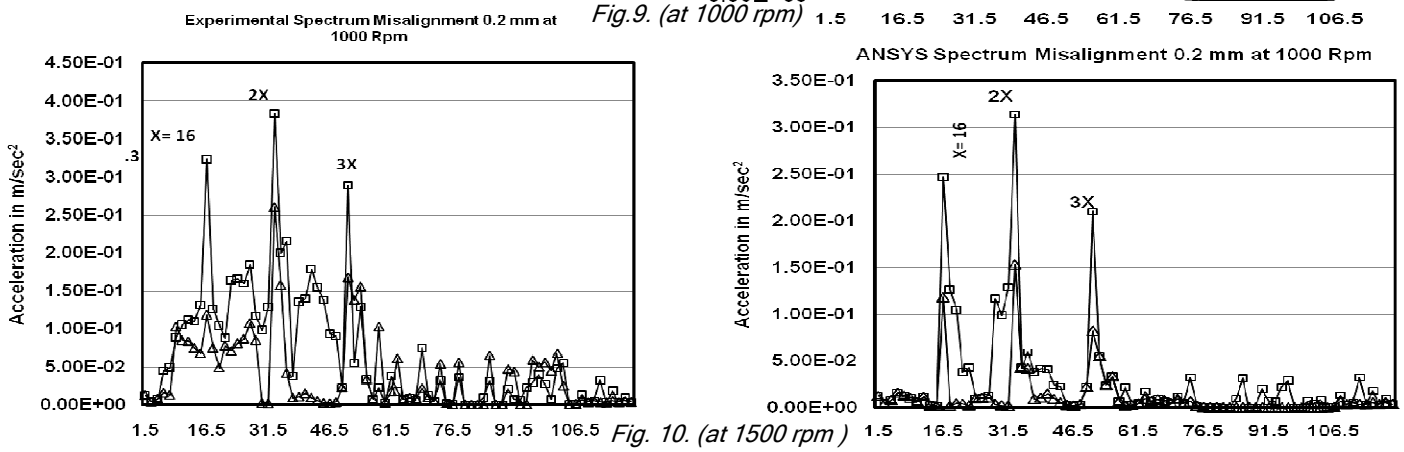

Fig. 10. (at 1500 rpm)

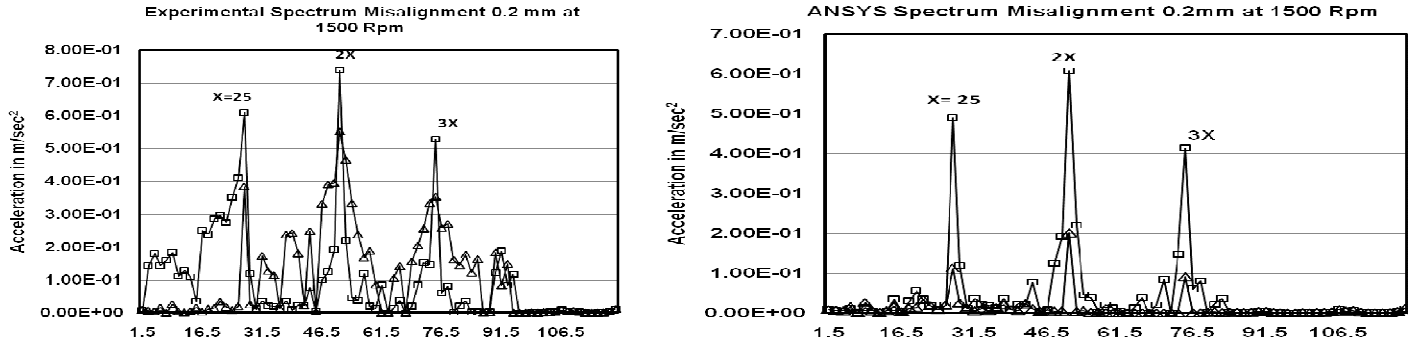

Fig.11. (at 2000 rpm)

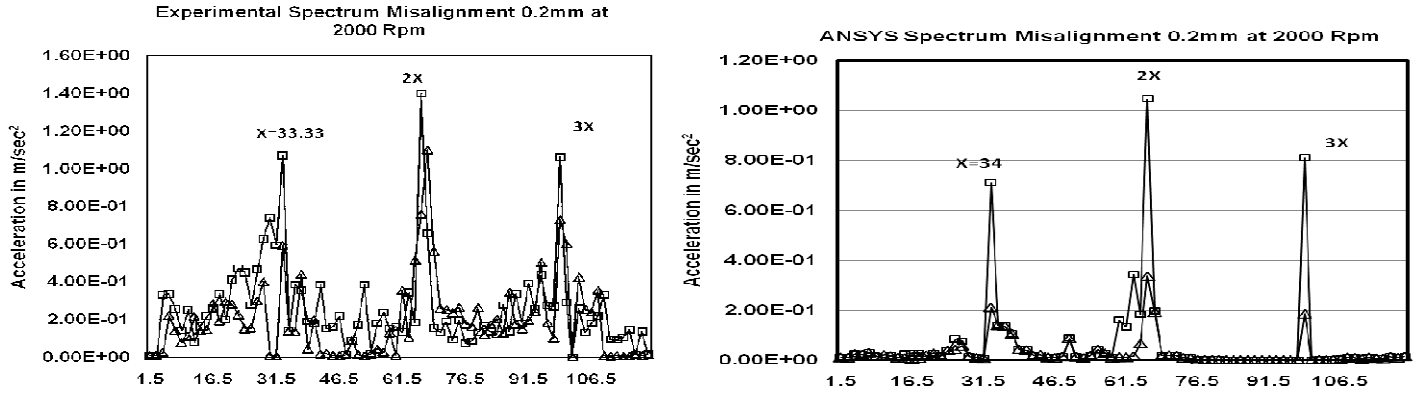

Indian Journal of Science and Technology Vol.2 No. 9 (Sep 2009) ISSN: 0974- 6846

Table 5. Acceleration (m/sec^2) values at different speeds (misalignment case)

RPM	ADASH Analyzer						ANSYS Results					
	Drive End			Non Drive End			Drive End			Non Drive End		
	1x	2x	3x	1x	2x	3x	1x	2x	3x	1x	2x	3x
500	0.023	**0.075**	0.054	0.05	**0.085**	0.059	0.028	**0.055**	0.031	0.043	**0.073**	0.04
1000	0.12	**0.256**	0.157	0.325	**0.39**	0.271	0.125	**0.156**	0.0575	0.25	**0.325**	0.22
1500	0.39	**0.523**	0.34	0.621	**0.75**	0.52	0.123	**0.221**	0.151	0.52	**0.63**	0.395
2000	0.61	**1.34**	0.631	1.2	**1.43**	1.17	0.22	**0.39**	0.23	0.72	**1.51**	0.82

The frequency spectra of all the four speeds shows that 2X shaft running speed is the predominant frequency indicating shaft misalignment and the experiment results are good agreement with the numerical (ANSYS) results. The misalignment case of 0.2 mm between driver and driven shaft results are shown in Table 5. Experimental results measured using vibration analyzer is compared with the ANSYS results.

Conclusion

The model of the pin type coupling-ball bearing system with misalignment was simulated. Throughout the experimental and simulation works, the validity of the model was successfully verified and the rotor dynamic characteristics related to misalignment were investigated. The experimental and simulated frequency spectra were obtained. Experimental predictions are good agreement with the numerical (ANSYS) results. Both the measured and numerical results spectra shows that misalignment can be characterized primarily two times shaft running speed (2X). However, misalignment (2X shaft running speed) effect is not close enough to one of the system natural frequencies to excite the system appreciably. Therefore in some case the misalignment response is hidden and does not show up in the vibration spectrum. On the other hand, if 2x shaft running speed is at or close to one of the system natural frequencies, the misalignment effect can be amplified and a high acceleration level at 2X shafts running speed is pronounced in the frequency spectrum.

Reference

1. Arumugam P, Swarnamani S and Prabhu BS (1995) Effects of coupling misalignment on the vibration characteristics of a two stage turbine rotor. *ASME Design Engg. Tech. Conf*. 84, 1049-1054.
2. Dewell DL and Mitchell LD (1984) Detection of a misaligned disk coupling using spectrum analysis. *ASME Trans. J. Vibration, Acoustics, Stress & Reliability Design*. 106, 9-16.
3. Ganeriwala S, Patel S and Hartung H (1999) The truth behind misalignment vibration spectra of rotating machinery. *Proc. Intl. Modal Analysis Conf*. pp: 2078-2205.
4. Gibbons CB (1976) Coupling misalignment forces. In: Proc. of the 5th Turbo Machinery Symposium, Gas Turbine Laboratories, Texas A&M Univ. pp: 111-116.
5. Goodman MJ (1989) Dynamics of rotor - bearing systems. London, Unwin Hyman Ltd.
6. Piotrowski J (2006) Shaft Alignment Handbook. Third Ed. Marcel Dekker, Inc. New York.
7. Sekhar AS and Prabhu BS (1995) Effects of coupling misalignment on Vibrations of rotating machinery. *J. Sound Vibration*. 185 (4), 655-671.
8. Simon G (1992) Prediction of vibration behavior of large turbo machinery on elastic foundation due to unbalance and coupling misalignment. Proc. of the Institution of Mechanical Engineers. *J. Mech. Engr*. 206, 29-39.
9. Vance JM (1988) Rotor dynamics of Turbomachinery. New York, John Wiley & Sons.
10. Xu M and Marangoni RD (1994a) Vibration analysis of a motor flexible coupling rotor system subject to misalignment and unbalance, part I: theoretical model and analyses. *J. Sound Vibration*. 176(5), 663-679.
11. Xu M and Marangoni RD (1994b) Vibration analysis of a motor flexible coupling rotor system subject to misalignment and unbalance, part II: Experimental validation. *J. Sound Vibration*. 176(5), 681-691.